Immobilization of Candida antarctica *Lipase on Nanomaterials and Investigation of the Enzyme Activity and Enantioselectivity*

Gülcan Coşkun, Zafer Çıplak, Nuray Yıldız & Ülkü Mehmetoğlu

Applied Biochemistry and Biotechnology

ISSN 0273-2289

Appl Biochem Biotechnol
DOI 10.1007/s12010-020-03443-2

Springer

Your article is protected by copyright and all rights are held exclusively by Springer Science+Business Media, LLC, part of Springer Nature. This e-offprint is for personal use only and shall not be self-archived in electronic repositories. If you wish to self-archive your article, please use the accepted manuscript version for posting on your own website. You may further deposit the accepted manuscript version in any repository, provided it is only made publicly available 12 months after official publication or later and provided acknowledgement is given to the original source of publication and a link is inserted to the published article on Springer's website. The link must be accompanied by the following text: "The final publication is available at link.springer.com".

Author's personal copy

Applied Biochemistry and Biotechnology
https://doi.org/10.1007/s12010-020-03443-2

Immobilization of *Candida antarctica* Lipase on Nanomaterials and Investigation of the Enzyme Activity and Enantioselectivity

Gülcan Coşkun[1] · Zafer Çıplak[1] · Nuray Yıldız[1] · Ülkü Mehmetoğlu[1]

Received: 11 May 2020 / Accepted: 29 September 2020/Published online: 06 October 2020
© Springer Science+Business Media, LLC, part of Springer Nature 2020

Abstract
This study defines the lipase immobilization protocol and enzymatic kinetic resolution of 1-phenyl ethanol with the use of immobilized lipases (LI) as a biocatalyst. Commercially available lipase *Candida antarctica B* (Cal-B) was immobilized onto graphene oxide (GO), iron oxide (Fe_3O_4) nanoparticles, and graphene oxide/iron oxide (GO/Fe_3O_4) nanocomposites. Characterization of pure and enzyme-loaded supports was carried out by scanning electron microscopy (SEM) and Fourier transform infrared (FTIR) spectroscopy. The influences of pH, temperature, immobilization time, crosslinker concentration, glutaraldehyde (GLA), epichlorohydrin (EPH), and surfactant concentrations (Tween 80 and Triton X-100) on the catalytic activity were evaluated for these three immobilized biocatalysts. The highest immobilized enzyme activities were 15.03 U/mg, 14.72 U/mg, and 13.56 U/mg for GO-GLA-CalB, Fe_3O_4-GLA-CalB, and GO/Fe_3O_4-GLA-CalB, respectively. Moreover, enantioselectivity and reusability of these immobilized lipases were compared for the kinetic resolution of 1-phenyl ethanol, using toluene as organic solvent and vinyl acetate as acyl donor. The highest values of enantiomeric excess ($ee_s = 99\%$), enantioselectivity ($E = 507.74$), and conversion ($c = 50.73\%$) were obtained by using lipase immobilized onto graphene oxide (GO-GLA-CalB). It was obtained that this enzymatic process may be repeated five times without important loss of enantioselectivity.

Keywords *Candida antarctica* lipase · Immobilization · Nanoparticles · Enzyme activity · Kinetic resolution

✉ Ülkü Mehmetoğlu
mehmet@eng.ankara.edu.tr

[1] Department of Chemical Engineering, Ankara University, Tandoğan, 06100 Ankara, Turkey

Author's personal copy

Introduction

Lipases (triacylglycerol acyl hydrolases, EC 3.1.1.3) are widely used enzymes in biocatalysts that have essential roles in organic chemistry since they have a broad specificity and can react with various substrates [1]. The solubility of lipases in water is very poor, that is why the reaction usually occurs at an aqueous-organic interface at which they perform better catalytic activity than at aqueous solution [2, 3]. Lipases can hydrolyze triglycerides at lipid-water interfaces since the hydrolytic reaction is reversible in a nonaqueous medium; they can also catalyze the formation of acylglycerols from glycerol and free fatty acids [4]. Applications of lipases in different industries have been steadily increasing, especially during the last few years. They have been used particularly in the food industry, in the pharmaceutical industry, in the pulp and paper industries, and in the chemical industries [5].

Enantioselectivity of the lipases has significant enzyme property for many applications, such as preparation of optically pure alcohols and esters, with a special interest in the pharmaceutical industry [6]. In order to produce bioactive compounds such as natural products, agrochemicals, and pharmaceuticals, enantiopure alcohols are significant constituents [7]. In a biological system, two enantiomers of a chiral compound may exhibit very distinct behaviors. Indeed, when a racemic mixture is used as a chiral drug, whose enantiomers display different biological effects, generally only one of the enantiomers is biologically active, whereas the other is either inactive or produces side-effects, including toxicity. For this reason, there has been a huge demand to produce optically pure drugs in the pharmaceutical industry [8–12]. Lipases generally exhibit better enantioselectivity in the kinetic resolution of secondary alcohols than in the kinetic resolution of primary or tertiary ones [13]. *Candida antarctica* lipase B (Cal-B) is a serine hydrolase and the most commonly used lipase compared with others [14]. Both its free and immobilized forms show very good activity and stability towards kinetic resolution of secondary alcohols [15]. Various studies have been published about the lipase-catalyzed kinetic resolution of 1-phenyl ethanol. In some of these studies, Cal-B was immobilized on different support materials or other lipases that have been used as biocatalysts. For example, in a recent study by Abahazi et al. [16], Cal-B was covalently immobilized onto bisepoxide-activated amino alkyl polymer resins, and then it was used to catalyze the kinetic resolution of 1-phenylethanol. They achieved high enantiomeric excess (ee > 99%) and enantioselectivity (E > 200) values. Also, the results represented that the immobilized enzyme can be used repeatedly and show long-term stability. In another work by Souza et al. [17], commercially available Cal-B (immobilized on a macroporous polyacrylate resin) was chosen as a biocatalyst for the kinetic resolution of 1-phenylethanol and high enantioselectivity (ee = 98, $E = 200$) was obtained.

In order to enhance the enantioselectivity and stability of an enzyme, there are different biochemical techniques. The most commonly used of these techniques is the immobilization of enzymes. A proper immobilization method can alter the selectivity of lipases and improve catalytic activity and biochemical properties [5, 18]. The use of immobilized enzymes as biocatalysts has drawn attention in recent years. They provide several advantages over their soluble forms; for example, they can be separated easily from the mixture, and they are generally more stable, enable production of pure products, have the ability to reuse the enzyme [19], increase storage stability, protect tertiary structure of enzyme [20], and minimize the inhibition by any environmental conditions [21].

Enzymes can be immobilized onto supports covalently via chemical interactions between active groups of the supports and amino acid groups of the enzyme molecules [13].

Author's personal copy

The immobilization of enzymes with covalent binding generally cause denaturation of enzyme and the loss of catalytic activity due to the limitation of conformational changes and generation of rigid structures along immobilization. On the other hand, the stability of enzymes will be increased considerably, and the leakage of the enzyme could be decreased [22]. Alternatively, it may be beneficial to utilize some additives such as substrates, ligands, and substrate analogues in order to protect the active center of the enzyme during the immobilization process. Therefore, when the active center of the enzyme captured by a substrate molecule, the conformational change of the enzyme can be reduced, and its catalytic activity can be protected during covalent binding [23]. During the covalent attachment procedure, the most critical point is the preference of a suitable solid support. Support materials should have high surface area and low cost; in addition, they should be environmentally friendly and nontoxic [24]. The interaction between enzyme and support material is a crucial factor since the properties of the support can modify the activity of the biocatalyst and enzyme loading [25].

There are many supports used for lipase immobilization, for example, a variety of nanostructures that provide low mass-transfer resistance and a large surface area, which upgrade binding efficiency, increase interaction with the enzyme, and develop the long-term storage and reusing of the enzyme [26]. The utilization of magnetite (Fe_3O_4) as a nanocarrier for the covalent immobilization of enzymes is notably promising since it has high surface area [27–29]; it allows recyclability and repeatability of biocatalysts having long-term stability [30], allows satisfactory separation under external magnetic fields [31], and supplies high enzyme loading per unit mass of support [32]. Another support material that can be used as an immobilization matrix is GO, which has attracted great attention on account of its definite chemical and surface properties [33]. Various functional groups such as C=O, -OH, -O- and -COOH in the structure of GO permit it to be hydrophilic and disperse easily in water and organic solvents. Thus, a suitable interaction occurs between graphene oxide and enzyme molecules [34, 35]. The combination of Fe_3O_4 nanoparticles with GO nanosheets offers another promising support material. Due to the very high surface area and strong interaction of GO nanosheets with Fe^{2+}/Fe^{3+} ions, Fe_3O_4 nanoparticles with small particle size and large surface area can easily prepared, separately. In addition, the Fe_3O_4 nanoparticles on GO nanosheets prevent the aggregation of the GO nanosheets and maintain the large surface area of the support material. Moreover, because of the excellent magnetic properties of Fe_3O_4 nanoparticles, the GO/Fe_3O_4 nanocomposite can separated easily with an external magnetic field. In the literature, there are some studies about the immobilization of different kind of lipases onto GO/Fe_3O_4 nanocomposite [36–38]. Xie and Huang [37] immobilized *Candida rugosa* lipase, and they obtained activity recovery as 64.9%. The immobilized enzyme was used to catalyze the transesterification of soybean oil with methanol.

In this study, it is aimed to increase the enzymatic activity and enantioselectivity of Cal-B by immobilizing it onto Fe_3O_4 nanoparticles, GO nanosheets and GO/Fe_3O_4 nanocomposite. For this purpose, GO, Fe_3O_4, and GO/Fe_3O_4 nanostructures were firstly prepared; subsequently, they were immobilized by covalent attachment of Cal-B and finally, the different immobilized samples were used as biocatalysts in the enantioselective transesterification reaction of (R, S)-1-phenylethanol for the first time in the literature. In addition, the reusability of the immobilized enzymes was examined; high catalytic activities of the enzymes were verified.

Author's personal copy

Materials and Methods

Materials

All chemicals were used without further purification. Lipase from *C. antarctica B* was provided by Novozymes. Graphite oxide was supplied by Graphene Company (Turkey). Ferrous chloride tetrahydrate ($FeCl_2$. $4H_2O$, 99%), ferric chloride hexahydrate ($FeCl_3$. $6H_2O$, 97%), glutaraldehyde (GA, %50 wt. in H_2O), epichlorohydrin (EPH), and Triton X-100 were obtained from Sigma-Aldrich. Calcium chloride ($CaCl_2$), sodium hydroxide (NaOH), toluene, hexane, 1-phenyl ethanol, 2-propanol, vinyl acetate, hydrochloric acid (HCl), tween 80, disodium hydrogen phosphate dihydrate ($Na_2HPO_4.2H_2O$), and monopotassium phosphate (KH_2PO_4) were purchased from Merck.

Synthesis of Nanostructures

Synthesis of Fe_3O_4 Nanoparticles

Fe_3O_4 nanoparticles were prepared by coprecipitation method in alkaline medium reported method in the literature [39]. The iron salts were dissolved in aqueous HCl (0.16 M) where the mole fraction of Fe^{2+} to Fe^{3+} was adjusted to 0.5. This solution was dropped into 1 M aqueous NaOH solution (50 ml) at 80 °C under the inert atmosphere. After 30-min strong mechanical stirring, the magnetic particles were collected by centrifugation at 10,000 rpm for 15 min. The particles were washed three times with deionized water and dried at 50 °C under vacuum for 24 h.

Preparation of GO Nanosheets

Preparation of GO was accomplished by ultrasonication of graphite oxide powder. Graphite oxide solution was subjected to ultrasonication at room temperature for 1 h. The brown dispersion was then centrifuged at 3000 rpm for 30 min to remove any unexfoliated graphite oxide [40].

Preparation of GO/Fe_3O_4 Nanocomposite

The GO/Fe_3O_4 nanocomposite was synthesized by an ultrasonic-assisted reverse coprecipitation method, according to literature [41], with some modifications. The above-obtained GO (0.2 g) was added to distilled water (25 ml), and the mixture was subjected to ultrasonication at room temperature for 30 min. The iron salts, $FeSO_4.7H_2O$ (0.48 g) and $FeCl_3.6H_2O$ (0.47 g) were dissolved in 25 mL of distilled water, followed by the addition of NaOH (1 M) to the iron salts suspension to adjust pH 4. Then, GO aqueous dispersion was added into the above suspension. Again, NaOH (1 M) was added dropwise to adjust pH from 4 to 10 in order to obtain black precipitates. After that, the resulted suspension sonicated at 60 °C for 45 min. Finally, the obtained black GO/Fe_3O_4 nanoparticles were collected by magnetic separation, washed with water, and then dried under vacuum at 50 °C.

Author's personal copy

Activation of the Supports

In this procedure, 20 mg support material was dissolved in 5 ml of phosphate buffer (PBS) (50 mM, pH 7.0), including Triton X-100 or Tween 80 surfactants at five different concentrations (10, 20, 30, 40, 50 mM). The mixture was sonicated at room temperature for 45 min then the aggregates were separated and washed with deionized water three times. The solution of ethylenediamine (2 ml) in phosphate buffer (50 mM, pH 7.0) was added, and the suspension was stirred at room temperature for 2 h [42]. The precipitates were separated and washed with deionized water three times. Next, 250 mM of GLA or EPH (150, 200, 250, and 300 mM) as cross-linker was added to the mixture and shaken (150 rpm, 30 °C, 4 h). Finally, the activated support materials were recovered from the suspension, washed three times with deionized water and dried at room temperature for 24 h.

Lipase Immobilization onto Activated Nanoparticles

Activated nanoparticles soaked into phosphate buffer (5 ml, 50 mM) at different pH medium (pH 5, pH 6, pH 7, pH 8) including Cal-B (1 ml). The immobilization process was carried out in a thermal shaker (150 rpm), with different contact times (8, 12, 16, 20, 24 h) and immobilization temperatures (20, 30, 40, 50, 60 °C). Finally, the supports were washed three times with phosphate buffer (50 mM, pH 7) and dried at room temperature for 24 h.

Enzyme Activity Measurement

In order to investigate the enzyme activity, low acidity high refined olive oil was chosen as a substrate. In a conical flax, olive oil (2 ml), $CaCl_2$ (0.1 M, 0.5 ml), phosphate buffer (0.07 M, pH 7, 3 ml), and deionized water (5 ml) were mixed and incubated in a thermal shaker (37 °C, 10 min, 150 rpm). After the incubation, native or immobilized lipase was added to the emulsion followed by reaction in a thermal shaker (37 °C, 20 min, 150 rpm). The acetone-ethyl alcohol mixture (1:1 v/v) was added to the reaction medium to terminate the reaction. Titration method with NaOH (0.02 M) was chosen to measure the amount of released free fatty acid. A unit (U) lipase activity is known as the amount of a standard lipase preparation that releases 1 mol of fatty acid equivalent per minute from the substrate emulsion under certain assay conditions. To calculate the specific activity of both native and immobilized lipases, Eq. 1 was used [43].

$$\text{Specific activity}\ (U/\text{mg}) = [(V_1/V_2) \times C \times 1000]/(t \times E) \quad (1)$$

where V_1 is the amount of consumed NaOH (for test) (ml), V_2 is the amount of consumed NaOH (for blank) (ml), C is concentration of NaOH (mol/l), E is amount of the enzyme (mg), and t is incubation time (min).

Enantioselective Transesterification of 1-Phenyl Ethanol with Immobilized Lipases

For enzymatic kinetic resolution, vinyl acetate (240 mM for GO-GLA-CalB and GO/Fe_3O_4 -GLA-CalB, 480 mM for Fe_3O_4 -GLA-CalB) and rac-1-phenyl ethanol (120 mM) were dissolved in organic solvent n-hexane (total reaction volume is 3 ml) in screw-capped vials. GO-GLA-CalB (15.33 U/mg), Fe_3O_4-GLA-CalB (14.26 U/mg), or GO/Fe_3O_4 -GLA-CalB (13.47 U/mg) and

Author's personal copy

molecular sieves (100 mg) were added to the mixture then stirred with constant shaking (150 rpm) at a fixed temperature (40 °C) in an orbital shaker. After the reaction, immobilized lipases were collected by filtering and organic solvent removed via rotary evaporator. The analysis of the samples was carried out by high-pressure liquid chromatography with a Chiral cell-OB column (4.6 mm × 50 mm, Daicel Chemical Ind. Ltd. France) using hexane: 2-propanol in the ratio of 95:05 at a flow rate of 0.90 ml/min and detected at 254 nm with a UV detector. The conversion (c) is described as fractional conversion [44]:

$$c = 1-([R] + [S])/([R]_0 + [S]_0) \quad (2)$$

where $[R]$ is the concentration of (R)-1-phenyletehanol, $[S]$ is the concentration of (S)-1-phenyletehanol, $[R]_0$ is the initial concentration of (R)-1-phenyletehanol, and $[S]_0$ is the initial concentration of (S)-1-phenyletehanol. The enantiomeric excess (ee%) percent and the enantiomeric ratio (E) was calculated [1]:

$$ee\% = ([R]-[S])/([R] + [S]) \quad (3)$$

$$E = \ln[(1-c)(1-ee)]/\ln[(1-c)(1 + ee)] \quad (4)$$

where c is conversion and ee% is the enantiomeric excess.

Results and Discussion

Characterization of the Nanostructures and Immobilized Lipases

Fourier Transform Infrared Spectroscopy Analysis

FTIR was utilized to analyze the efficiency of covalent immobilization. Figure 1a. shows the FTIR spectra of pure GO and enzyme immobilized GO. The spectrum of GO shows the broadband at 3410 cm^{-1} that assigned to O-H stretching vibrations of the C-OH groups, the band at 1737 cm^{-1} shows C=O stretching vibrations of the carbonyl and carboxylic groups and the absorption band at 1620 cm^{-1} because of the existence of C=C or demonstrates the skeletal vibrations due to unoxidized graphitic domains [45, 46]. The spectra of Cal-B immobilized GO clearly indicate the following bands: 3425 cm^{-1} (O-H, NH_2) due to water and Cal-B, 1647 cm^{-1} (C=O) corresponding to Amid I, 1550 cm^{-1} corresponding to Amid II bands of C-N stretching vibrations and N-H bending. Figure 1b shows FTIR spectra of pure Fe_3O_4 and lipase immobilized Fe_3O_4. It can be seen that before lipase immobilization onto Fe_3O_4, the Fe-O vibrations of Fe_3O_4 centered at 695 cm^{-1}, after Cal-B immobilization this peak shifted to 650 cm^{-1} due to the interaction of enzyme and Fe_3O_4 nanoparticles. The large and broad band is detected at 3423 cm^{-1} demonstrating the existence of both the OH and NH_2 groups of water and Cal-B molecules [32]. Amide I band is the most intense absorption band of proteins that gives a peak at 1643 cm^{-1}. It is caused by the stretching vibrations of the C-N (from 10% to 20%) and C=O groups (from 70 to 85%) [47]. Amid II band is attributed to the N-H bending and C-N stretching vibrations at 1550 cm^{-1}. The presence of several characteristic peaks of GO/Fe_3O_4 such as Fe-O vibrations (573 cm^{-1}), C–OH stretching vibration (1217 cm^{-1}) [48], aromatic C=C stretching (1600 cm^{-1}) and oxygen stretching vibrations (3440 cm^{-1}) show the

Author's personal copy

successful preparation of GO/Fe_3O_4 nanocomposite (Fig. 1c). After enzyme immobilized onto the support, the bands corresponded to chemical structure of enzyme was appeared at 1061 cm^{-1} (C-N stretching vibrations for aliphatic amines), 1550 cm^{-1} (Amid II), 1647 cm^{-1} (Amid I band), 2353–2357 cm^{-1} (the adsorption doublet band of CO_2), and 3440 cm^{-1} (O-H and N-H absorption). The spectroscopic examination verifies that the enzyme Cal-B was successfully immobilized on the surface of supports.

Scanning Electron Microscopy Analysis

Figure 2 shows the SEM images of the supports before and after enzyme immobilization. The smooth and regular surface of initial GO/Fe_3O_4 and Fe_3O_4 support can be seen in Fig. 2a, c respectively. After lipase immobilized, the irregular surface of the supports can be visualized in Fig. 2b, d shows that the supports are filled unevenly by the lipase.

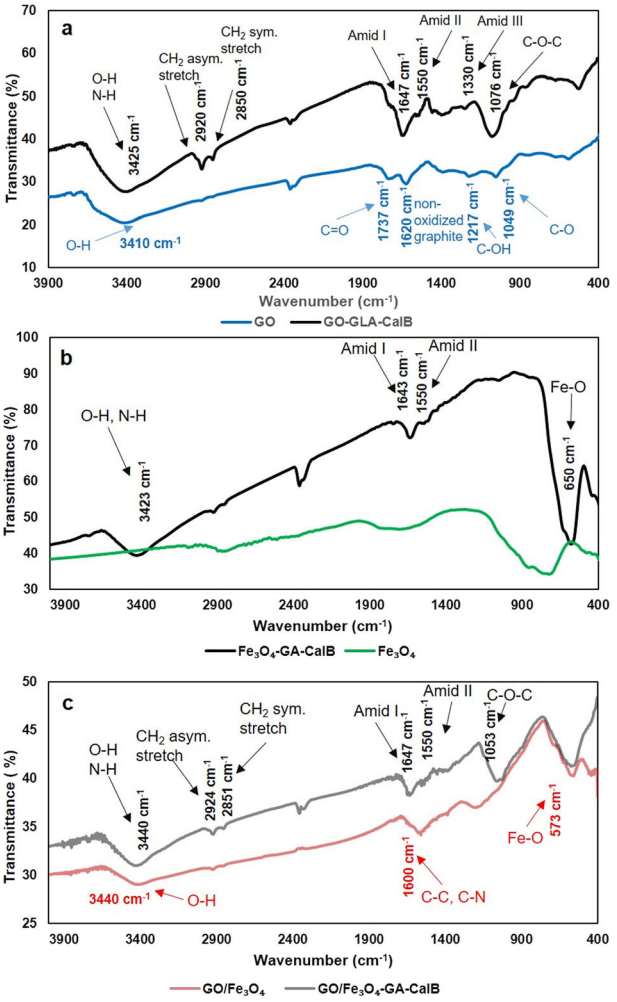

Fig. 1 FTIR spectrum of **a** pure GO and enzyme immobilized GO, **b** pure Fe_3O_4 and enzyme immobilized Fe_3O_4, **c** GO/Fe_3O_4 and enzyme immobilized GO/Fe_3O_4

Author's personal copy

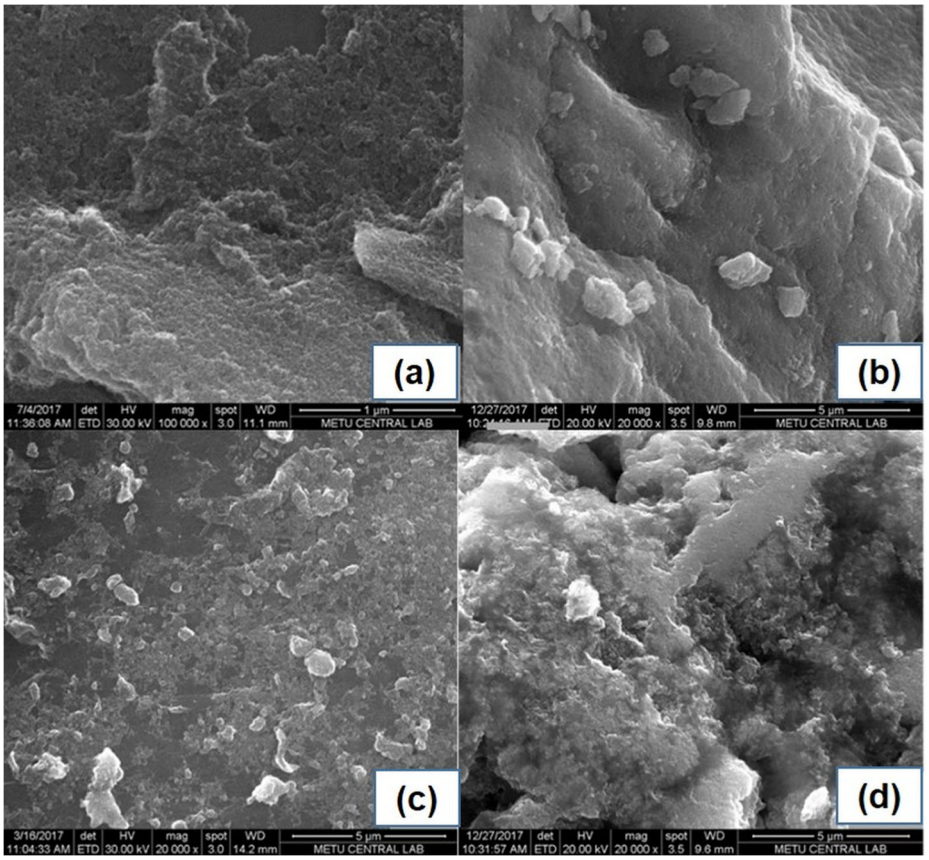

Fig. 2 SEM images of **a** GO/Fe_3O_4 before lipase immobilization; **b** GO/Fe_3O_4 after lipase immobilization; **c** Fe_3O_4 before lipase immobilization; **d** GO/Fe_3O_4 after lipase immobilization

The Effect of pH and Temperature on Immobilization

One of the most important parameters that cause alteration of the enzyme activity in aqueous solutions is pH. The pH change of the medium during immobilization affects the tertiary structure and active site of the enzyme molecules [49]. To determine the impact of pH on immobilization, activation of the supports (with crosslinkers, 30 °C, 4 h) and the immobilization of Cal-B onto the supports (30 °C, 12 h) were carried out at various pH values (pH 5–8). The effect of pH on the immobilization protocol is shown in Fig. 3a. The highest enzyme activity was obtained at pH 6 (13.29 U/mg) for GO-GLA-CalB enzyme, at pH 7 (11.85 U/mg) for Fe_3O_4-GLA-CalB and at pH 8 (12.96 U/mg) for GO/Fe_3O_4-GLA-CalB.

When these values are compared with the free enzyme activity (18.52 U/mg, pH 6, 37 °C) in the optimum conditions, it can be seen that the activities of three immobilized enzymes decreased. The relative activities of immobilized samples are 72%, 64%, and 70% for GO-GLA-CalB, Fe_3O_4-GLA-CalB, and GO/Fe_3O_4-GLA-CalB, respectively. The pH values demonstrate that there is no significant conformational change in the GO-GLA-CalB (pH 6) and Fe_3O_4-GLA-CalB (pH 7) enzymes during covalent binding.

Author's personal copy

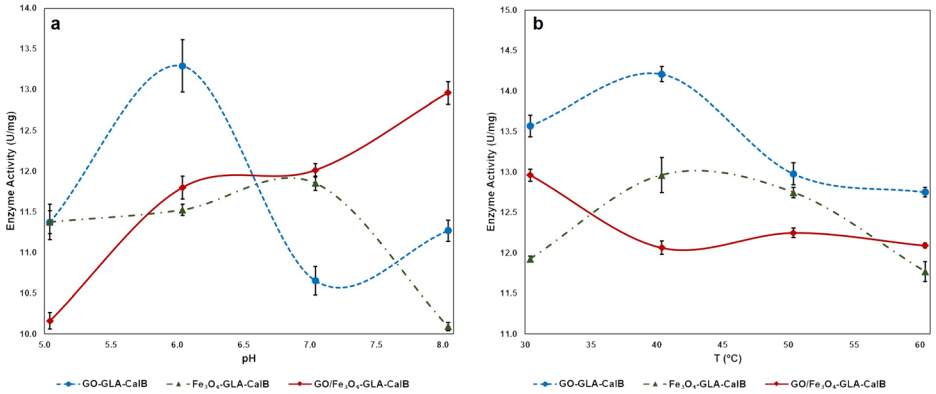

Fig. 3 **a** Effect of pH on immobilized enzyme activity. Reaction conditions: GLA (250 mM), Cal-B (1 ml), PBS (50 mM), $t_{immobilization}$ (12 h), T (30 °C), **b** effect of temperature on immobilized enzyme activity. Reaction conditions: GLA (250 mM), Cal-B (1 ml), PBS (50 Mm, pH 7), $t_{immobilization}$ (12 h)

However, the results represent that lipase immobilized onto GO/Fe_3O_4-GLA-CalB exhibits higher resistance to pH (pH 8.0). Miletic et al. [50] found similar result in their study for Cal-B immobilized on polystyrene nanoparticles. In order to observe the effect of reaction temperature on immobilization, the activation of the supports and the immobilization protocol were carried out at different temperatures (30–60 °C, pH 7.0), and the results are shown in Fig. 3b. The optimum reaction temperature of the free lipase is 30 °C, while the immobilized enzymes represent the best catalytic activities at 40 °C. At this temperature, the relative activities of GO-GLA-CalB, Fe_3O_4-GLA-CalB, and GO/Fe_3O_4-GLA-CalB are 74.2%, 81.4%, and 75.15%, respectively. Activity recovery of *Candida rugosa* enzyme immobilized onto GO/Fe_3O_4 nanocomposite was obtained as 64.9% by Xie and Huang [37]. According to these results, their resistance to thermal denaturation is better than the free lipase. As the result of the immobilization, molecules have limited conformational mobility, thus stability is increased against various deactivating forces. Similar values were obtained by Yılmaz et al. [51] when the *Candida rugosa* lipase (CRL) was encapsulated within chemically inert sol-gel composite matrixes. The main reason of the improved stabilitiy is the covalent bonds between the enzyme and the matrix, which restrict the conformational mobility of the molecules and cause the rigidity and stability of the enzyme to increase [52].

The reaction time is very important for enzyme immobilization. If there is an insufficient interaction, the enzyme cannot bind on the support or the enzyme may be denatured because of a longer duration of the interaction.

Figure 4 shows the catalytic activity of immobilized lipases prepared at various immobilization times. As seen in Fig. 4, it is clear that the catalytic activities of the three immobilized enzymes are different for all immobilization times. Fe_3O_4-GLA-CalB shows the best activity for 16 h. At this time, the catalytic activity of Fe_3O_4-GLA-CalB is 13.73 U/mg. However, the catalytic activities decreased after 16 h. This phenomenon can be related to denaturation of lipases at a long time. Optimum immobilization time for GO-GLA-CalB and GO/Fe_3O_4-GLA-CalB is 12 h at which the activities are 14.17 U/mg and 13.12 U/mg, respectively. Longer time slightly reduced the immobilization yield on the support. It could be concluded that the

Author's personal copy

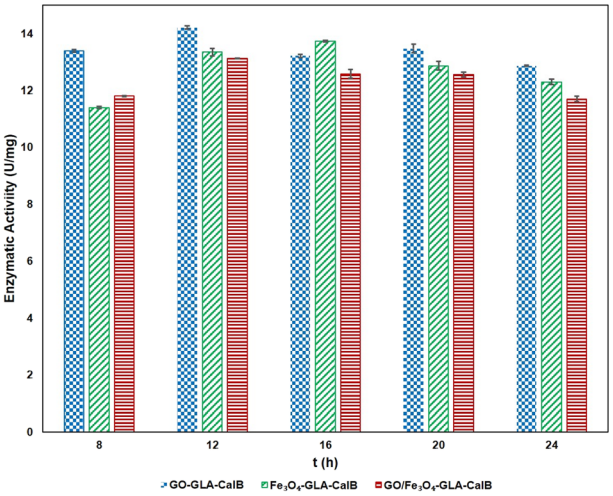

Fig. 4 The effect of immobilization time on enzyme activity

immobilized enzymes have different structures and show different activities at different immobilization times.

The Effect of Crosslinkers Concentration on the Catalytic Activity

Enzyme immobilization by covalent binding generally includes two steps. First, the support surface is activated using bifunctional agents, and then the enzyme is immobilized on the activated surface covalently. Crosslinkers, often used in covalent binding, behave as a bridge between the support material and enzyme molecules [53]. In this part of the study, activation of the supports was carried out with varying quantities of GLA and EPH (150, 200, 250, and 300 mM) for 4 h at 30 °C. Then, the free enzyme was immobilized onto these activated supports as previously mentioned. When GO was activated by glutaraldehyde, with the increasing of glutaraldehyde concentration the activity of immobilized enzyme increased, after 250 mM (2.36%, v/v) of glutaraldehyde concentration the activity decreased. When Fe_3O_4 was activated with glutaraldehyde, the highest immobilized enzyme activity was obtained when 300 mM (2.83%, v/v) of glutaraldehyde was used. For GO/Fe_3O_4 support material, 200 mM (1.90%, v/v) of glutaraldehyde represented the highest enzyme activity, after 200 mM (1.90%, v/v) of glutaraldehyde the activity decreased. The three immobilized lipases gain different conformations from each other after the immobilization protocol; therefore, their highest activities are detected at different glutaraldehyde concentrations. However, for each sample, with the increasing GLA concentration, the enzyme activity increased because of the increased concentration of aldehyde groups on the support surfaces. On the other hand, after a certain GLA concentration, the activities of the immobilized preparations were decreased, at a high GLA concentration, the multiple chemical bonds might be generated between the support material and the enzyme molecules [54]. When the carriers were activated with epichlorohydrin at different concentrations, it was observed that enzyme activities were lower than

Author's personal copy

glutaraldehyde (Table 1). The results prove glutaraldehyde is more effective than epichlorohydrin on the enzymatic activity.

The Effect of Surfactants on Enzyme Activity

The existence of surfactants during immobilization increases the thermal and chemical stability of enzymes [55, 56]. The effect of increasing concentration of non-ionic surfactants Triton X-100 and Tween 80 were analyzed in this study, and the results were presented in Table 2. In the same conditions, without the use of surfactants, the activity of enzyme immobilized on GO, Fe_3O_4 and GO/Fe_3O_4 were 15.33, 14.26, and 13.47 U/mg, respectively (Table 1). When 30 mM (3.7% v/v) and 40 mM (4.9%, v/v) of Tween 80 were used, the highest immobilized enzyme activities were 15.03, 14.72, and 13.56 U/mg for GO-GLA-CalB, Fe_3O_4-GLA-CalB, and GO/Fe_3O_4-GLA-CalB, respectively. The higher concentration of the surfactants caused the decrease in the activity of all three immobilized enzymes. The similar behavior was also observed when Triton X-100 was used as the surfactant. However, the increase in concentration for both surfactants did not have a significant effect on immobilized enzyme activities. There are two possible considerations to explain why there is no significant change in enzyme activity: (i) The interaction time (45 min) between the surfactants, and the support materials is insufficient. (ii) The use of surfactants during the activation process of the support material rather than the enzyme immobilization process.

Enantioselective Transesterification of 1-Phenyl Ethanol with Immobilized Lipases

In this study, Cal-B immobilized onto three nanostructures, and the immobilized lipases, Fe_3O_4-GLA-CalB, GO-GLA-CalB, and GO/Fe_3O_4-GLA-CalB, catalyzed the transesterification of 1-phenyl ethanol with vinyl acetate when used in hexane with the activity of 15.33 U/mg, 14.26 U/mg, and 13.47 U/mg, respectively (Table 1). Enantioselective transesterification of 1-phenylethanol assayed for three immobilized enzymes for different reaction times. As shown in Fig. 5a, b, and c enantioselectivity is considerably influenced by the different immobilized enzymes. Fe_3O_4-GLA-CalB showed poor enantioselectivity (ee% = 23.00, $E = 3.77$) with 31.36% conversion in 15 h. Significant changes observed when lipases GO-GLA-CalB and GO/Fe_3O_4-GLA-CalB catalyzed the reaction. The highest values of enantioselectivity ($E = 507.74$, 375.77), enantiomeric excess (ee > 99%, 94.32%), and conversion ($c = 50.73\%$, 49.02%) were obtained when GO-GLA-CalB and GO/Fe_3O_4-GLA-CalB catalyzed the reaction, respectively. This is probably due to the fact that enzymes with different conformations and physical properties that obtained by the immobilization of Cal-B onto

Table 1 The effect of glutaraldehyde and epichlorohydrin concentrations on the activity of the immobilized enzyme

Immobilized enzyme activity, U/mg	GO-CalB		Fe_3O_4-CalB		GO/Fe_3O_4-CalB	
Cross linker concentration, mM	GLA	EPH	GLA	EPH	GLA	EPH
150	13.47	12.28	13.46	11.81	13.03	11.70
200	14.45	13.44	13.83	12.98	13.47	12.41
250	15.33	13.59	14.26	12.46	13.12	12.53
300	15.24	14.22	14.45	13.16	11.85	11.69

Author's personal copy

Table 2 The effect of surfactant concentration on the activity of the immobilized enzyme

Immobilized enzyme activity, U/mg	GO-GLA-CalB		Fe_3O_4-GLA-CalB		GO/Fe_3O_4-GLA-CalB	
Surfactant concentration, mM	Tween 80	Triton X-100	Tween 80	Triton X-100	Tween 80	Triton X-100
10	14.45	13.99	13.92	13.83	13.03	13.29
20	14.57	14.00	14.35	13.52	13.33	13.47
30	15.03	14.57	14.72	14.04	13.46	13.53
40	14.58	14.63	14.34	14.35	13.56	13.70
50	14.04	13.44	14.04	14.23	12.71	13.34

different support materials. Since the enzyme is attached directly to the support material, the supports having different morphological and physical properties affect the catalytic properties of the enzyme [26, 57]. Thus, the support material used in the immobilization affects the biological activity of the enzyme by altering the properties of the enzyme [58].

Operational Stability

When the best immobilization conditions, support material, and immobilization method are selected, the activity and the stability of the immobilized enzyme relative to the free enzyme

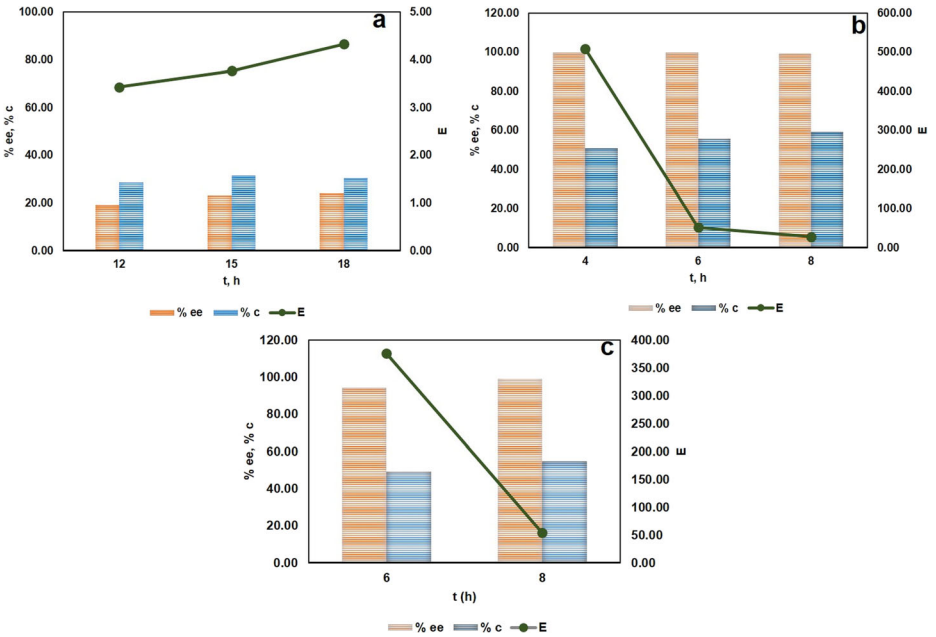

Fig. 5 Enantioselectivity of different lipases for kinetic resolution of 1-phenyl ethanol **a** Fe_3O_4-GLA-CalB (14.26 U/mg), $C_{(R, S)\text{-1-phenyl-ethanol}} = 120$ mM, $C_{\text{Vinyl acetate}} = 480$ mM, Org. solvent = Hexane, $V_{\text{tot}} = 3$ ml, $M_{\text{molecular sieve}} = 100$ mg, $T = 40$ °C. **b** GO-GLA-CalB (15.33 U/mg), $C_{(R, S)\text{-1-phenyl-ethanol}} = 120$ mM, $C_{\text{Vinyl acetate}} = 240$ mM, Org. solvent = Hexane, $V_{\text{tot}} = 3$ ml, $M_{\text{molecular sieve}} = 100$ mg, $T = 40$ °C. **c** GO/Fe_3O_4-GLA-CalB (13.47 U/mg), $C_{(R, S)\text{-1-phenyl-ethanol}} = 120$ mM, $C_{\text{Vinyl acetate}} = 480$ mM, Org. solvent = Hexane, $V_{\text{tot}} = 3$ ml, $M_{\text{molecular sieve}} = 100$ mg, $T = 40$ °C ee% = (S-R)/(S + R)] × 100, c% = [1 − ((S + R)/(S_0 + R_0))] × 100, $E = [\ln((1 - c)(1 - ee))/\ln((1 - c)(1 + ee))]$

Author's personal copy

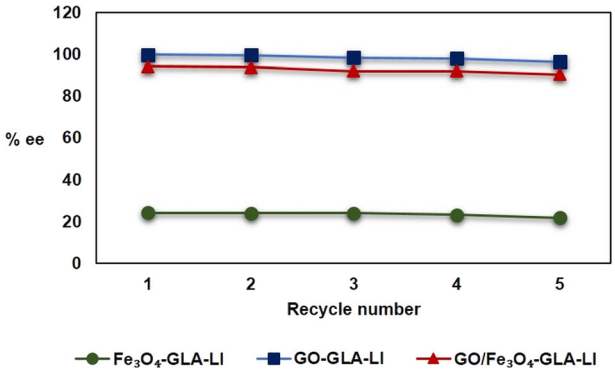

Fig. 6 Reusability of immobilized enzymes

may increase. Recovery and repeated reusability of immobilized enzymes in catalytic systems are another important parameters. To determine the reuse of immobilized enzymes subsequent cycles for three immobilized enzymes were carried out separately. Each of them was used for different reaction conditions, but each cycle was carried out on the same conditions of reactions. After the first and further reaction cycles of the kinetic resolution of 1-phenylethanol, the immobilized lipases were regained from the reaction medium with the use of a magnet or via filtration and washed 3 times with hexane. Then, they were dried to remove the organic solvent, and they were used in the new reaction system. The experiment was repeated up to five reaction cycles with the same immobilized lipases.

Figure 6 shows the reusability of immobilized enzymes on Fe_3O_4, GO and GO/Fe_3O_4. It is seen that there is no significant decrease in enantiomeric ratios and this enzymatic process can be repeated five times without important loss of enantioselectivity.

Conclusion

Immobilization of Cal-B onto GO, Fe_3O_4, and GO/Fe_3O_4 was accomplished with glutaraldehyde by covalent immobilization. The three forms of the immobilized enzymes, the relative activities of them were between 70 and 80%. The enantioselectivity of Cal-B immobilized onto Fe_3O_4 was rather poor. However, *Candida antarctica* lipase immobilized covalently onto GO and GO/Fe_3O_4 nanoparticles can be efficiently used for enantioselective transesterification of R, S-1-phenyl ethanol with vinyl acetate as acyl donor and hexane as organic solvent. The reactions carried out excellent conversion (50.73%, 49.02%) along with excellent ee (> 99%, 94.32%) and *E* (507.74, 375.77) in 4, 6 h for the enzymes immobilized onto GO and GO/Fe_3O_4, respectively. These ee and *E* values are higher than the results in the literature. Moreover, the results presented that the immobilized lipase could be used repeatedly for different catalytic systems, which is an economically important advantage.

Compliance with Ethical Standards

Conflict of Interest The authors declare that they have no conflict of interest.

Author's personal copy

References

1. Dhake, K. P., Deshmukh, K. M., Wagh, Y. S., Singhal, R. S., & Bhanage, B. M. (2012). Investigation of steapsin lipase for kinetic resolution of secondary alcohols and synthesis of valuable acetates in non-aqueous reaction medium. *Journal of Molecular Catalysis B: Enzymatic, 77*, 15–23. https://doi.org/10.1016/J.MOLCATB.2012.01.009.
2. Adlercreutz, P. (2013). Immobilisation and application of lipases in organic media. *Chemical Society Reviews, 42*(15), 6406–6436. https://doi.org/10.1039/C3CS35446F.
3. Ghanem, A., & Aboul-Enein, H. Y. (2004). Lipase-mediated chiral resolution of racemates in organic solvents. *Tetrahedron: Asymmetry, 15*(21), 3331–3351. https://doi.org/10.1016/J.TETASY.2004.09.019.
4. Alloue, W. A. M., Destain, J., Amighi, K., & Thonart, P. (2007). Storage of Yarrowia lipolytica lipase after spray-drying in the presence of additives. *Process Biochemistry, 42*(9), 1357–1361. https://doi.org/10.1016/J.PROCBIO.2007.05.024.
5. Homaei, A. A., Sariri, R., Vianello, F., & Stevanato, R. (2013). Enzyme immobilization: an update. *Journal of Chemical Biology, 6*(4), 185–205. https://doi.org/10.1007/s12154-013-0102-9.
6. Qayed, W. S., Aboraia, A. S., Abdel-Rahman, H. M., & Youssef, A. F. (2015). Lipases-catalyzed enantioselective kinetic resolution of alcohols. *Journal of Chemical and Pharmaceutical Research, 7*(5).
7. Singh, M. N., Hemant, K. S. Y., Ram, M., & Shivakumar, H. G. (2010). Microencapsulation: a promising technique for controlled drug delivery. *Research in pharmaceutical sciences, 5*(2), 65–77.
8. Hernández-Fernández, F. J., de los Ríos, A. P., Tomás-Alonso, F., Gómez, D., & Víllora, G. (2008). Kinetic resolution of 1-phenylethanol integrated with separation of substrates and products by a supported ionic liquid membrane. *Journal of Chemical Technology & Biotechnology, 84*(3), 337–342. https://doi.org/10.1002/jctb.2044.
9. Xian-ming, H., & Jun, L. (1999). Optically active alcohols: resolution and synthesis from asymmetric reduction of prochiral ketones. *Wuhan University Journal of Natural Sciences, 4*(2), 205–210. https://doi.org/10.1007/BF02841502.
10. Frings, K., Koch, M., & Hartmeier, W. (1999). Kinetic resolution of 1-phenyl ethanol with high enantioselectivity with native and immobilized lipase in organic solvents. *Enzyme and Microbial Technology, 25*(3–5), 303–309. https://doi.org/10.1016/S0141-0229(99)00044-7.
11. Leitgeb, M., & Knez, Ž. (2009). Optimization of (R, S)-1-phenylethanol kinetic resolution over Candida antarctica lipase B in ionic liquids. *Journal of Molecular Catalysis B-enzymatic - J MOL CATAL B-ENZYM, 58*, 24–28.
12. de Miranda, A. S., Miranda, L. S. M., & de Souza, R. O. M. A. (2015). Lipases: valuable catalysts for dynamic kinetic resolutions. *Biotechnology Advances, 33*(5), 372–393. https://doi.org/10.1016/j.biotechadv.2015.02.015.
13. Barbosa, O., Ariza, C., Ortiz, C., & Torres, R. (2010). Kinetic resolution of (R/S)-propranolol (1-isopropylamino-3-(1-naphtoxy)-2-propanolol) catalyzed by immobilized preparations of Candida antarctica lipase B (CAL-B). *New Biotechnology, 27*(6), 844–850. https://doi.org/10.1016/j.nbt.2010.07.015.
14. Alves, J. S., Garcia-Galan, C., Schein, M. F., Silva, A. M., Barbosa, O., Ayub, M. A. Z., et al. (2014). Combined effects of ultrasound and immobilization protocol on butyl acetate synthesis catalyzed by CALB. *Molecules (Basel, Switzerland), 19*(7), 9562–9576. https://doi.org/10.3390/molecules19079562.
15. Raza, S., Fransson, L., & Hult, K. (2001). Enantioselectivity in Candida antarctica lipase B: a molecular dynamics study. *Protein science : a publication of the Protein Society, 10*(2), 329–338. https://doi.org/10.1110/ps.33901.
16. Abahazi, E., Lestal, D., Boros, Z., & Poppe, L. (2016). Tailoring the spacer arm for covalent immobilization of Candida antarctica lipase B-thermal stabilization by Bisepoxide-activated aminoalkyl resins in continuous-flow reactors. *Molecules (Basel, Switzerland), 21*(6). https://doi.org/10.3390/molecules21060767.
17. de Souza, R. O. M. A., Antunes, O. A. C., Kroutil, W., & Kappe, C. O. (2009). Kinetic resolution of rac-1-phenylethanol with immobilized lipases: a critical comparison of microwave and conventional heating protocols. *The Journal of Organic Chemistry, 74*(16), 6157–6162. https://doi.org/10.1021/jo9010443.
18. Raharjo, T. J., Febrina, L., Wardoyo, F. A., & Swasono, R. T. (2016). Effect of deacetylation degree of chitosan as solid support in lipase immobilization by glutaraldehyde crosslink. *Asian Journal of Biochemistry, 11*(3), 127–134. https://doi.org/10.3923/ajb.2016.127.134.
19. Costa, H. C., Romão, B. B., Ribeiro, E. J., Miriam, M., & Resende. (2013). Glutaraldehyde effect in the immobilization process of alpha-galactosidase from Aspergillus niger in the ion exchange resin duolite A-568.
20. Önal, S., & Telefoncu, A. (2003). Comparison of chitin and amberlite IRA-938 for α-galactosidase immobilization. *Artificial Cells, Blood Substitutes, and Biotechnology, 31*(1), 19–33. https://doi.org/10.1081/BIO-120018001.

Author's personal copy

21. Kuo, C.-H., Liu, Y.-C., Chang, C.-M. J., Chen, J.-H., Chang, C., & Shieh, C.-J. (2012). Optimum conditions for lipase immobilization on chitosan-coated Fe3O4 nanoparticles. *Carbohydrate Polymers, 87*(4), 2538–2545. https://doi.org/10.1016/J.CARBPOL.2011.11.026.
22. Jian, H., Wang, Y., Bai, Y., Li, R., & Gao, R. (2016). Site-specific, covalent immobilization of dehalogenase ST2570 catalyzed by formylglycine-generating enzymes and its application in batch and semi-continuous flow reactors. *Molecules (Basel, Switzerland), 21*(7). https://doi.org/10.3390/molecules21070895.
23. Ozturk, T. K., & Kilinc, A. (2010). Immobilization of lipase in organic solvent in the presence of fatty acid additives. *Journal of Molecular Catalysis B: Enzymatic, 67*(3–4), 214–218. https://doi.org/10.1016/J.MOLCATB.2010.08.008.
24. Zucca, P., Fernandez-Lafuente, R., & Sanjust, E. (2016). Agarose and its derivatives as supports for enzyme immobilization. *Molecules (Basel, Switzerland), 21*(11). https://doi.org/10.3390/molecules21111577.
25. Pinto, M. C. C., Freire, D. M. G., & Pinto, J. C. (2014). Influence of the morphology of core-shell supports on the immobilization of lipase B from Candida antarctica. *Molecules (Basel, Switzerland), 19*(8), 12509–12530. https://doi.org/10.3390/molecules190812509.
26. Mohamad, N. R., Marzuki, N. H. C., Buang, N. A., Huyop, F., & Wahab, R. A. (2015). An overview of technologies for immobilization of enzymes and surface analysis techniques for immobilized enzymes. *Biotechnology and Biotechnological Equipment, 29*(2), 205–220. https://doi.org/10.1080/13102818.2015.1008192.
27. Yang, D., Wang, X., Shi, J., Wang, X., Zhang, S., Han, P., & Jiang, Z. (2016). In situ synthesized rGO–Fe3O4 nanocomposites as enzyme immobilization support for achieving high activity recovery and easy recycling. *Biochemical Engineering Journal, 105*, 273–280. https://doi.org/10.1016/j.bej.2015.10.003.
28. Shi, X., Xu, J., Lu, C., Wang, Z., Xiao, W., & Zhao, L. (2019). Immobilization of high temperature-resistant GH3 β-glucosidase on a magnetic particle Fe3O4-SiO2-NH2-Cellu-ZIF8/zeolitic imidazolate framework. *Enzyme and Microbial Technology*. https://doi.org/10.1016/j.enzmictec.2019.05.004.
29. Zhao, J.-f., Lin, J.-p., Yang, L.-r., & Wu, M.-b. (2019). Enhanced performance of Rhizopus oryzae lipase by reasonable immobilization on magnetic nanoparticles and its application in synthesis 1,3-diacyglycerol. *Applied Biochemistry and Biotechnology, 3*(188), 677–689. https://doi.org/10.1007/s12010-018-02947-2.
30. Juang, T.-Y., Kan, S.-J., Chen, Y.-Y., Tsai, Y.-L., Lin, M.-G., & Lin, L.-L. (2014). Surface-functionalized hyperbranched poly(amido acid) magnetic nanocarriers for covalent immobilization of a bacterial gamma-glutamyltranspeptidase. *Molecules (Basel, Switzerland), 19*(4), 4997–5012. https://doi.org/10.3390/molecules19044997.
31. Song, J., Su, P., Yang, Y., & Yang, Y. (2017). Efficient immobilization of enzymes onto magnetic nanoparticles by DNA strand displacement: a stable and high-performance biocatalyst. *New Journal of Chemistry, 41*(14), 6089–6097. https://doi.org/10.1039/C7NJ00284J.
32. Khoshnevisan, K., Vakhshiteh, F., Barkhi, M., Baharifar, H., Poor-Akbar, E., Zari, N., et al. (2017). Immobilization of cellulase enzyme onto magnetic nanoparticles: applications and recent advances. *Molecular Catalysis, 442*, 66–73. https://doi.org/10.1016/J.MCAT.2017.09.006.
33. Cipolatti, E. P., Valério, A., Henriques, R. O., Moritz, D. E., Ninow, J. L., Freire, D. M. G., et al. (2016). Nanomaterials for biocatalyst immobilization-state of the art and future trends. *RSC Advances*. https://doi.org/10.1039/c6ra22047a.
34. Yadav, M., Rhee, K. Y., Park, S. J., & Hui, D. (2014). Mechanical properties of Fe3O4/GO/chitosan composites. *Composites Part B: Engineering, 66*, 89–96. https://doi.org/10.1016/J.COMPOSITESB.2014.04.034.
35. Zhou, L., Jiang, Y., Ma, L., He, Y., & Gao, J. (2014). Immobilization of glucose oxidase on polydopamine-functionalized graphene oxide. *Applied Biochemistry and Biotechnology, 2*(175), 1007–1017. https://doi.org/10.1007/s12010-014-1324-1.
36. Shao, Y., Jing, T., Tian, J., & Zheng, Y. (2015). Graphene oxide-based Fe3O4 nanoparticles as a novel scaffold for the immobilization of porcine pancreatic lipase. *RSC Advances, 126*(5), 103943–103955. https://doi.org/10.1039/c5ra19276e.
37. Xie, W., & Huang, M. (2018). Immobilization of Candida rugosa lipase onto graphene oxide Fe3O4 nanocomposite: characterization and application for biodiesel production. *Energy Conversion and Management, 159*, 42–53. https://doi.org/10.1016/j.enconman.2018.01.021.
38. Mosayebi, M., Salehi, Z., Doosthosseini, H., Tishbi, P., & Kawase, Y. (2020). Amine, thiol, and octyl functionalization of GO-Fe3O4 nanocomposites to enhance immobilization of lipase for transesterification. *Renewable Energy*. https://doi.org/10.1016/j.renene.2020.03.040.
39. Atila Dinçer, C., Yıldız, N., Aydoğan, N., & Çalımlı, A. (2014). A comparative study of Fe3O4 nanoparticles modified with different silane compounds. *Applied Surface Science, 318*, 297–304. https://doi.org/10.1016/J.APSUSC.2014.06.069.

Author's personal copy

40. Li, D., Müller, M. B., Gilje, S., Kaner, R. B., & Wallace, G. G. (2008). Processable aqueous dispersions of graphene nanosheets. *Nature Nanotechnology, 3*, 101.
41. Chang, Q., Huang, J., Ding, Y., & Tang, H. (2016). Catalytic oxidation of phenol and 2,4-dichlorophenol by using horseradish peroxidase immobilized on graphene oxide/Fe3O4. *Molecules, 21*(8).
42. Sikora, A., Chełminiak-Dudkiewicz, D., Siódmiak, T., Tarczykowska, A., Sroka, W. D., Ziegler-Borowska, M., & Marszałł, M. P. (2016). Enantioselective acetylation of (R,S)-atenolol: the use of *Candida rugosa* lipases immobilized onto magnetic chitosan nanoparticles in enzyme-catalyzed biotransformation. *Journal of Molecular Catalysis B: Enzymatic, 134*, 43–50. https://doi.org/10.1016/J.MOLCATB.2016.09.017.
43. Rosu, R., Uozaki, Y., Iwasaki, Y., & Yamane, T. (1997). Repeated use of immobilized lipase for monoacylglycerol production by solid-phase glycerolysis of olive oil. *Journal of the American Oil Chemists' Society, 74*(4), 445–450. https://doi.org/10.1007/s11746-997-0104-2.
44. Kramer, M., Cruz, J. C., Pfromm, P. H., Rezac, M. E., & Czermak, P. (2010). Enantioselective transesterification by Candida antarctica lipase B immobilized on fumed silica. *Journal of Biotechnology, 150*(1), 80–86. https://doi.org/10.1016/J.JBIOTEC.2010.07.018.
45. Tolasz, J., Štengl, V., & Ecorchard, P. (2014). The preparation of composite material of graphene oxide–polystyrene. *Environment, Chemistry and Biology : Selected, peer review papers from the 2014 3rd International Conference on Environment, Chemistry and Biology (ICECB 2014) November 29–30,2014, Mauritius*.
46. Yang, F., Zhao, M., Zheng, B., Xiao, D., Wu, L., & Guo, Y. (2012). Influence of pH on the fluorescence properties of graphene quantum dots using ozonation pre-oxide hydrothermal synthesis. *Journal of Materials Chemistry, 22*(48), 25471–25479. https://doi.org/10.1039/C2JM35471C.
47. Sahare, P., Ayala, M., Vazquez-Duhalt, R., & Agrawal, V. (2014). Immobilization of peroxidase enzyme onto the porous silicon structure for enhancing its activity and stability. *Nanoscale Research Letters, 9*(1), 409. https://doi.org/10.1186/1556-276X-9-409.
48. Narayanan, T. N., Liu, Z., Lakshmy, P. R., Gao, W., Nagaoka, Y., Sakthi Kumar, D., et al. (2012). Synthesis of reduced graphene oxide–Fe3O4 multifunctional freestanding membranes and their temperature dependent electronic transport properties. *Carbon, 50*(3), 1338–1345. https://doi.org/10.1016/J.CARBON.2011.11.005.
49. Xu, M.-H., Kuan, I.-C., Deng, F.-Y., Lee, S.-L., Kao, W.-C., & Yu, C.-Y. (2016). Immobilization of lipase from Candida rugosa and its application for the synthesis of biodiesel in a two-step process. *Asia-Pacific Journal of Chemical Engineering, 11*(6), 910–917. https://doi.org/10.1002/apj.2025.
50. Miletic, N., Abetz, V., Ebert, K., & Loos, K. (2010). Immobilization of Candida antarctica lipase B on polystyrene nanoparticles. *Macromolecular Rapid Communications, 31*(1), 71–74. https://doi.org/10.1002/marc.200900497.
51. Yilmaz, E., Sezgin, M., & Yilmaz, M. (2011). Immobilization of *Candida rugosa* lipase on magnetic sol–gel composite supports for enzymatic resolution of (R,S)-Naproxen methyl ester. *Journal of Molecular Catalysis B: Enzymatic, 69*(1–2), 35–41. https://doi.org/10.1016/J.MOLCATB.2010.12.007.
52. İspirli Doğaç, Y., & Teke, M. (2013). Immobilization of bovine catalase onto magnetic nanoparticles. *Preparative Biochemistry & Biotechnology, 43*. https://doi.org/10.1080/10826068.2013.773340.
53. Nguyen, H. H., & Kim, M. (2017). An overview of techniques in enzyme immobilization. *Applied Science and Convergence Technology, 26*(6), 157–163. https://doi.org/10.5757/ASCT.2017.26.6.157.
54. Zhu, J., & Sun, G. (2012). Lipase immobilization on glutaraldehyde-activated nanofibrous membranes for improved enzyme stabilities and activities. *Reactive and Functional Polymers, 72*(11), 839–845. https://doi.org/10.1016/J.REACTFUNCTPOLYM.2012.08.001.
55. Soto, D., Escobar, S., Guzmán, F., Cárdenas, C., Bernal, C., & Mesa, M. (2017). Structure-activity relationships on the study of β-galactosidase folding/unfolding due to interactions with immobilization additives: Triton X-100 and ethanol. *International Journal of Biological Macromolecules, 96*, 87–92. https://doi.org/10.1016/J.IJBIOMAC.2016.12.026.
56. de Oliveira, U. M. F., de Matos, L. J. B., de Souza, M. C. M., Pinheiro, B. B., dos Santos, J. C. S., & Gonçalves, L. R. B. (2018). Effect of the presence of surfactants and immobilization conditions on catalysts' properties of Rhizomucor miehei lipase onto chitosan. *Applied Biochemistry and Biotechnology, 184*(4), 1263–1285. https://doi.org/10.1007/s12010-017-2622-1.
57. Ali Khan, A., & Alzohairy, M. A. (2010). Recent advances and applications of immobilized enzyme technologies: a review. *Research Journal of Biological Sciences, 5*(8), 565–575. https://doi.org/10.3923/rjbsci.2010.565.575.
58. Spahn, C., & Minteer, S. D. (2008). Enzyme immobilization in biotechnology. *Recent Patents on Engineering, 2*(3), 195–200. https://doi.org/10.2174/187221208786306333.

Publisher's Note Springer Nature remains neutral with regard to jurisdictional claims in published maps and institutional affiliations.